

Compatibility Studies of Valsartan with Different Pharmaceutical Excipients

IOANA CRISTINA TITA¹, LAVINIA LUPA², BOGDAN TITA^{3*}, ROXANA LIANA STAN⁴, LAURA VICAS^{1,5}

¹Carol Davila University of Medicine and Pharmacy, Faculty of Pharmacy, 6 Traian Vuia Str., 020956, Bucharest, Romania

²Politehnica University Timisoara, Faculty of Industrial Chemistry and Environmental Engineering, 2 Victoriei Sq., 300006, Timisoara, Romania

³Vasile Goldis Western University of Arad, Faculty of Pharmacy, Department of Pharmaceutical Sciences, 86 L. Rebreanu Str., 300041, Arad, Romania

⁴University of Medicine and Pharmacy Iuliu Hatieganu, Faculty of Pharmacy, 13 Emil Isaac Str., 400023, Cluj-Napoca, Romania

⁵ University of Oradea, Faculty of Medicine and Pharmacy, Speciality of Pharmacy, 29 Nicolae Jiga Str., 410028, Oradea, Romania

Compatibility studies between active drugs and excipients are substantial in the pharmaceutical technology. Thermal analysis has been extensively used to obtain information about drug-excipient interactions and to perform pre-formulation studies of pharmaceutical dosage forms. The objective of the present study was to evaluate the compatibility of the valsartan (VALS) with pharmaceutical excipients of common use including diluents, binders, disintegrants, lubricants and solubilising agents. Thermogravimetry (TG), derivative thermogravimetry (DTG), but especially differential scanning calorimetry (DSC) were used for a first screening to find small variations in peak temperature and/or their associated enthalpy for six drug/excipient mixtures (starch, cross carameloze sodique, microcrystalline cellulose 102, povidone K30, lactose monohydrate and magnesium stearate), which indicate some degree of interaction. Additional methods using Fourier transformed infrared spectroscopy (FT-IR) and X-ray powder diffraction (XRPD) confirmed the incompatibility of VALS with starch, povidone K30, lactose monohydrate and magnesium stearate. Those excipients should be avoided in the development of solid dosage forms.

Keywords: drug-excipient compatibility, valsartan, simultaneous TG/DTG/DSC

Cardiovascular disease is one of the most common chronic diseases in clinic; it causes high morbidity and mortality worldwide. When hearts suffer stress, the *cardiac remodelling* characterized by typical pathological cardiac hypertrophy occurs, resulting in heart failure [1].

Valsartan (VALS) (fig. 1), N-(1-oxopentyl)-N-[[2'-(1H-tetrazol-5-yl) [1,1'-bi-phenyl]-4-yl]methyl]-L-valine, is a selective angiotensin II type 1 receptor blocker indicated for the treatment of hypertension [2].

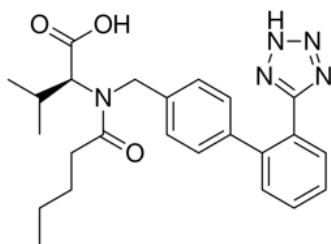


Fig. 1. Chemical structure of Valsartan

Valsartan is a kind of anti-hypertensive drug and licensed for the treatment of patients with symptomatic heart failure, and it plays an important role in the process of heart failure injury [3].

The study of drug-excipient compatibility is an important stage in the development of a solid dosage form as their incompatibility can alter the stability and/or the bioavailability of drugs, thereby, affecting its safety and/or efficacy. Two types of chemical incompatibilities have been described between excipients and drugs: those corresponding to intrinsic chemical drug degradation such hydrolysis or oxidation but without significant direct covalent chemical reactions, and those corresponding to covalent reaction between the drug and the excipient [4,5].

Thermal analysis is a very useful technique for evaluating a range of different samples of the same

material, to assess the influence of excipients on the physico-chemical properties of pharmaceutical materials and pharmaceutical dosage forms [6-9].

Throughout the different thermal methods reported on drug-excipient compatibility studies, DSC has been shown to be a rapid, sensitive and simple technique used in routine experiments. Small variations in peak temperature or associated enthalpy are interpreted as an indication of interaction and possible incompatibility [10-12].

Despite the advantages of DSC there are certain limitations. The extrapolation of findings obtained at high temperatures, are not always in agreement with the drug real situation in the formulation. Therefore, the DSC results must be interpreted carefully and some complementary techniques, such as Fourier transformed infrared spectroscopy (FT-IR) and X-ray powder diffraction (XRPD) can be useful in avoiding misleading conclusions [13-17].

In our previous papers we provided the importance of the thermal analysis in estimation on the thermal behaviour of different pharmaceuticals, respectively their possible interaction with excipients [18-21].

In this work, the characterization and the compatibility of valsartan (VALS) with six different pharmaceutical excipients of common use in the development of solid dosage forms was evaluated. For this purpose, simultaneous TG/DTG and especially DSC measurements were carried out on each of the components, both in the pure form and the corresponding 1:1 (w/w) physical mixtures. FT-IR spectroscopy and X-ray powder diffraction (XRPD) were used as complementary techniques to adequately implement and assist in interpretation of the DSC results.

*email: bogdantita@yahoo.com, Phone: 0722879279

Experimental part

Materials and samples

The valsartan (VALS), active substance, was obtained from Polisano Pharma SRL, (lot: VT0020911) as pure compound, able to be used for medical purpose.

The excipients were as follows: corn starch hydrated (Roquette Freres, France, lot: E1209); crosscarmelose sodique (CCS), microcrystalline cellulose PH 102 (MC 102) from J. Rettenmaier & Sohne GmbH, Germany (lot: 5610273320); polyvinylpyrrolidone K30 (PVP K30 or PVP) from BASF Aktiengesellschaft, Germany (lot: 95658675LO); lactose monohydrate (α -lactose) from Friesland Foods Domo, Holland (lot: 620831); colloidal silicon dioxide (SiO_2C) from Degussa AG, Germany (lot: 3157040314) and magnesium stearate (MS) from Undesa, Spain (lot: 484931).

Physical mixtures of VALS with each selected excipient were prepared in the 1:1 (w:w) ratio by simple mixture of the components in an agate mortar with pestle for approximately 5 min. The 1:1 (w/w) ration was chosen in order to maximise the probability of observing any interaction.

Methods

Thermal analysis

The TG/DTG/DSC curves were recorded using a Netzsch-STA 449 TG/DTA instrument in the temperature range of 20-1000 °C, under a dynamic atmosphere of nitrogen ($20 \text{ mL} \times \text{min}^{-1}$) and at a heating rate (β) of $10 \text{ }^\circ\text{C} \times \text{min}^{-1}$, using platinum crucibles and weighed samples of approximately 20 mg of samples.

Fourier transformed infrared spectroscopy (FT-IR) and X-ray diffraction

FT-IR spectra of drug, excipients and grinding mixtures were recorded on a Shimadzu Prestige 21 apparatus using KBr stressed discs in the range of $4000\text{-}400 \text{ cm}^{-1}$.

X-ray diffraction patterns (XRPD), for the same category of substances, were obtained with a Rigaku Ultima IV diffractometer using CuK_α radiation.

Results and discussions

Thermal behaviour of VALS

The thermoanalytical curves of VALS are presented in figure 2.

In the temperature range 25-96 °C, VALS eliminates the absorbed water ($\Delta m = 1.10\%$ and $T_{\text{peak DTG}} = 68.2 \text{ }^\circ\text{C}$). The nature of the process is endothermic and $T_{\text{peak DSC}} = 68.2 \text{ }^\circ\text{C}$.

Continuing the TG/DTG curves indicates a thermal stability of the VALS, while the DSC curve shows an endothermic peak ($T_{\text{peak DSC}} = 113.9 \text{ }^\circ\text{C}$), which corresponds to the melting of valsartan.

Thermal decomposition of VALS results in three distinct steps on the TG/DTG curves.

The first decomposition step takes place in the temperature range 174-275 °C, with $T_{\text{peak DTG}} = 215.5 \text{ }^\circ\text{C}$ and $\Delta m = 12.74\%$. The DSC curve appears a bit broader, exothermic in nature, with $T_{\text{peak DSC}} = 235.5 \text{ }^\circ\text{C}$.

After some thermal stability, the decomposition continued in the range 309 - 544 °C, with $T_{\text{peak DTG}} = 403.3 \text{ }^\circ\text{C}$ and $\Delta m = 68.88\%$. On the DSC curve appears a small endothermic pic, relatively small, with $T_{\text{peak DSC}} = 408.1 \text{ }^\circ\text{C}$.

Thermal decomposition continues in the third stage (544 - 871 °C), with $T_{\text{peak DTG}} = 744.4 \text{ }^\circ\text{C}$ and $\Delta m = 17.28\%$. This latter process is accompanied by a large endothermic DSC curve with $T_{\text{peak DSC}} = 703.0 \text{ }^\circ\text{C}$.

Compatibility study with excipients

Thermal analysis in general and DSC in particular have been proposed to be rapid methods for evaluating physico-chemical interactions between components of a formulation by comparing curves obtained for 1:1 (w:w) physical mixtures and thus selecting suitable excipients with compatibility corresponding to.

Figures 3, 4 and 5 show the TG, DTG and DSC curves of the substances used in the compatibility study. Each curve shows a specific behaviour, depending on the characteristics of each excipient.

On the TG/DTG curves of starch there is a first mass loss ($\Delta m = 11.90\%$) in the temperature range 35 - 137 °C, with $T_{\text{peak DTG}} = 70.4 \text{ }^\circ\text{C}$. Mass loss corresponds to the removal of water from the hydrated starch. This process is endothermic, highlighted on the DSC curve, with $T_{\text{peak DSC}} = 81.5 \text{ }^\circ\text{C}$.

The thermal decomposition of starch is a relatively complex process, which takes place in two stages, partially distinct. The first stage, the main one, with $\Delta m = 69.20\%$, takes place in the range 255 - 397 °C, and the DTG curve appears a bit sharp, with $T_{\text{peak DTG}} = 314.8 \text{ }^\circ\text{C}$. At the same time, two peaks of endothermic nature appear on the DSC curve:

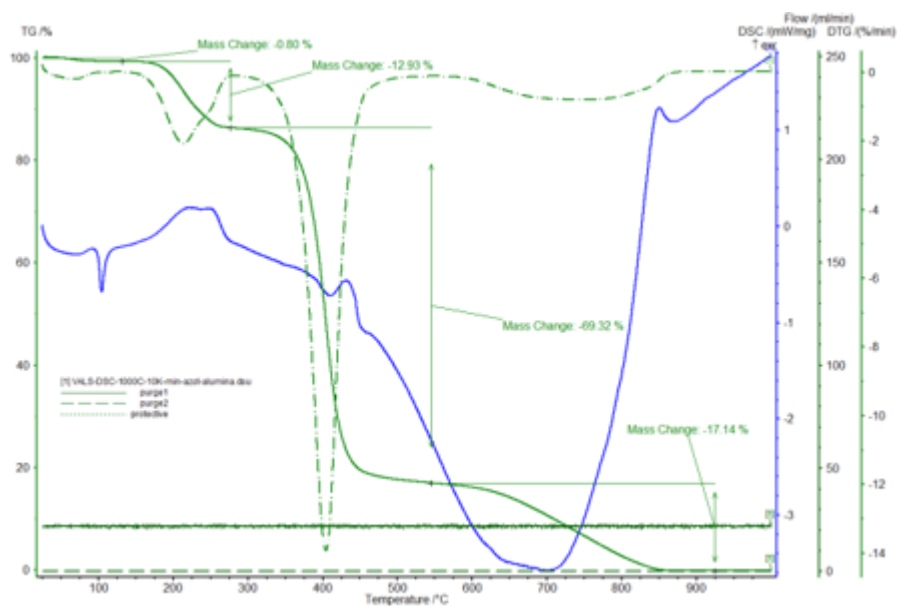


Fig. 2. TG/DTG/DSC curves of pure VALS

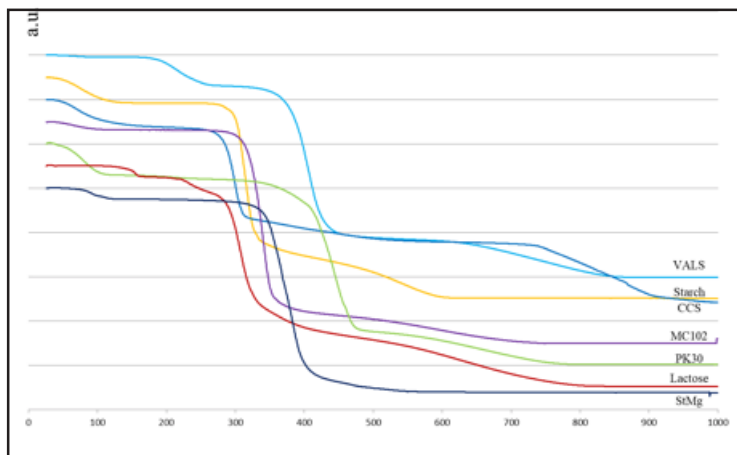


Fig. 3. TG curves of all substances used in compatibility study

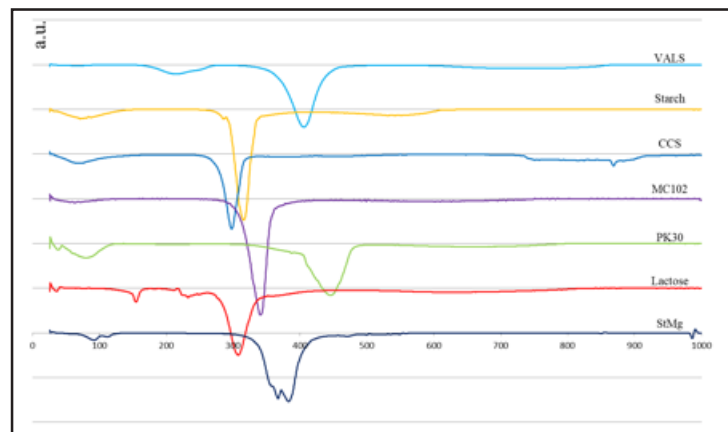


Fig. 4. DTG curves of all substances used in compatibility study

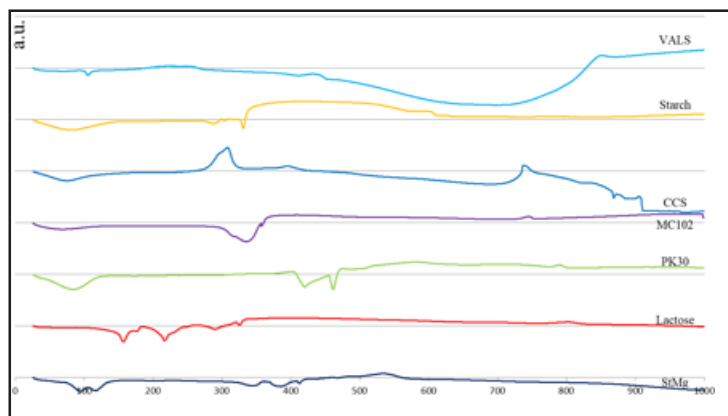


Fig. 5. DSC curves of all substances used in compatibility study

- a slightly smaller first, with $T_{\text{peak DSC}} = 286.7\text{ }^{\circ}\text{C}$, accompanied by a shoulder on the right side at $306.8\text{ }^{\circ}\text{C}$;

- the second bigger, sharp, appears at a temperature of $329.6\text{ }^{\circ}\text{C}$.
In the second decomposition step, corresponding to the range $397 - 625\text{ }^{\circ}\text{C}$, the mass loss is 18.9% , and on the DTG curve appears a bit wide, with $T_{\text{peak DTG}} = 544.4\text{ }^{\circ}\text{C}$. On the DSC curve two small peaks of endothermic nature at temperatures of $580.0\text{ }^{\circ}\text{C}$, respectively $610.4\text{ }^{\circ}\text{C}$.

The thermal behaviour of croscarmellose sodium is interesting from the point of view of the nature of the thermal effects of thermal decomposition but also of the complex decomposition process itself.

In the temperature range $25 - 187\text{ }^{\circ}\text{C}$, with $T_{\text{peak DTG}} = 68.2\text{ }^{\circ}\text{C}$, dehydration takes place. Mass loss is 12.70% , and the DSC curve shows an endothermic peak, with $T_{\text{peak DSC}} = 75.6\text{ }^{\circ}\text{C}$.

Thermal decomposition begins immediately after the $187\text{ }^{\circ}\text{C}$ temperature, in a first step ($187 - 598\text{ }^{\circ}\text{C}$), with a bit sharp, on the DTG curve and $T_{\text{peak DTG}} = 299.5\text{ }^{\circ}\text{C}$. The mass loss is 51.80% , and the DSC curve shows two peaks of exothermic nature:

- the first high relative, sharp, at $307.4\text{ }^{\circ}\text{C}$;

- second smaller, at $395.6\text{ }^{\circ}\text{C}$.
The decomposition process continues in the range $598 - 1000\text{ }^{\circ}\text{C}$, with a mass loss of 27.30% and a residual mass of 8.60% . Corresponding to the above process, on the DTG curve is present a little wide peak, with $T_{\text{peak DTG}} = 865.1\text{ }^{\circ}\text{C}$, while on the DSC curve a relatively large, relatively exothermic peak of $737.0\text{ }^{\circ}\text{C}$ appears, followed by two small peaks of an endothermic nature at $865.1\text{ }^{\circ}\text{C}$, respectively $894.1\text{ }^{\circ}\text{C}$.

In the case of microcrystalline cellulose 102, the first process that takes place on heating is the elimination of adsorbed water ($\Delta m = 3.89\%$) in the temperature range $38 - 125\text{ }^{\circ}\text{C}$. On the DTG curve, this process corresponds to a relatively large and not very large, with $T_{\text{peak DTG}} = 63.0\text{ }^{\circ}\text{C}$. Obviously, on the DSC curve this process is characterized by an endothermic peak, with $T_{\text{peak DSC}} = 70.4\text{ }^{\circ}\text{C}$.

No other thermal phenomenon is noticeable before thermal decomposition begins between $263 - 479\text{ }^{\circ}\text{C}$, respectively $479 - 774\text{ }^{\circ}\text{C}$.

In the first stage, as a percentage of lost weight ($\Delta m = 89.60\%$), two sharp, high peaks with $T_{\text{peak DTG}} = 340.7^\circ\text{C}$, respectively $T_{\text{peak DSC}} = 337.0^\circ\text{C}$, appear on the DTG and DSC curves, the latter being of nature endothermic.

The second stage has a mass loss of only 6.48%, and the DTG curve does not actually show a peak, with the mass variation taking place around the temperature of 625.0°C . The DSC curve shows a peak of exothermic nature with $T_{\text{peak DSC}} = 742.9^\circ\text{C}$.

The first process evidenced by the thermal curves of povidone K30 corresponds to the dehydration process. This takes place in the temperature range $37 - 133^\circ\text{C}$, with $T_{\text{peak DTG}} = T_{\text{peak DSC}} = 80.0^\circ\text{C}$, and the nature of the phenomenon is endothermic. The loss of water is 14.60% and the water is easily removed, but the total mass of lost water depends on the moisture content of the atmosphere (eg dry or wet N_2). Also, the shape of the DSC peak (its width) depends on the relative humidity of the atmosphere above the sample. Apparently, dehydration is complete at 137°C in N_2 . However, a secondary water loss step ($\Delta m = 2.20\%$) starts after 137°C and is complete around 319°C . There are no significant peaks on the DTG and DSC curves. Thermal analysis SEM and XRPD all show that the compound is in a vitreous phase with a glass transition near 200°C .

The thermal decomposition takes place in the temperature ranges $319-504^\circ\text{C}$, respectively $504-813^\circ\text{C}$.

The first step ($319-504^\circ\text{C}$) implies a mass loss of 69.10%, and a sharp high peak with a $T_{\text{peak DTG}} = 442.2^\circ\text{C}$ is present on the DTG curve, while on the DSC curve two high endothermic peaks and sharpened at 414.8°C , respectively 457.7°C .

The second step ($504-813^\circ\text{C}$), with a mass loss of 16.10%, shows a wide peak on the DTG curve, with the so-called maximum at 657.7°C , and on the DSC curve two peaks: the first of exothermic nature at 575.0°C and the second endothermic at 774.0°C .

The amorphous (100%) form of lactose can be identified by thermal analysis, more precisely based on the DSC technique, whose curve exhibits an exothermic peak at 167°C , which represents the transformation of the amorphous form into crystalline form. It is hatched by two endothermic peaks, one at 210°C and the other at 216°C . These peaks correspond to the melting of α -lactose (lactose monohydrate), respectively β -lactose (anhydrous lactose), which means that the two forms are present in different proportions.

Also, 100% crystalline lactose, according to the XRPD method, contains forms α and β .

According to the thermogram, the water content (4.88%) of lactose monohydrate is maintained at about 165°C . Practically, water is removed between 127 and 167°C , with $T_{\text{peak DTG}} = 150.3^\circ\text{C}$. Water loss is accompanied by a strong endothermic effect on DSC curve ($T_{\text{peak DSC}} = 151.8^\circ\text{C}$).

There is then a slight loss of mass ($\Delta m = 1.00\%$), the compound being stable to about 215°C , after which it decomposes. Prior to decomposition, melting of lactose (in fact α -lactose) occurs, the process being characterized by a strong endothermic peak ($T_{\text{peak DSC}} = 214^\circ\text{C}$). Immediately after melting, in the range of $215-259^\circ\text{C}$, with $T_{\text{peak DTG}} = 232.6^\circ\text{C}$ and a loss of weight of 6.48%, decomposition of β -lactose (present along with α -lactose) occurs. This process is accompanied on the DSC curve by a high endothermal sharp peak ($T_{\text{peak DSC}} = 215.5^\circ\text{C}$).

After these processes the actual decomposition takes place, the so-called main process, a complex one, which takes place in two stages.

The first step takes place between 259 and 513°C , with a high peak on the DTG curve, having a $T_{\text{peak DTG}} = 304.5^\circ\text{C}$. On the DSC curve there are two sufficiently large, endothermic, respectively exothermic peaks with the appropriate temperatures: $T_{\text{peak DSC endo}} = 289.5^\circ\text{C}$ and $T_{\text{peak DSC exp}} = 319.2^\circ\text{C}$. The mass loss is 68.00%.

The decomposition process continues with the second stage, in the temperature range $513-835^\circ\text{C}$, characterized by a broad peak on the DTG curve, with $T_{\text{peak DTG}} = 625.0^\circ\text{C}$.

Like the DTG curve, the DSC curve indicates the complexity of the process and the relatively wide temperature range in which it occurs by the emergence of two small peaks of exothermic nature at 698.0°C , respectively 723.0°C , as well as by the occurrence of a significant exothermic peak, with $T_{\text{peak DSC}} = 800.0^\circ\text{C}$. The loss of mass suffered is 20.50%.

In the case of colloidal SiO_2 , in the temperature range $33 - 144^\circ\text{C}$, a small mass loss ($\Delta m = 1.08\%$) occurs on the TG curve due to the probable and possible humidity adsorbed, especially due to the area of the specific surface area. The DSC curve shows an endothermic peak, with $T_{\text{peak DSC}} = 51.2^\circ\text{C}$. Next, up to 400°C , no mass variation occurs, but a small endothermic peak with $T_{\text{peak DSC}} = 337.7^\circ\text{C}$ appears on the DSC curve. The presence of this peak may be due to a phenomenon of physical nature, insignificant, however.

In the temperature range $400-1000^\circ\text{C}$ there is a slight decrease in mass ($\Delta m = 0.92\%$), and on the DSC curve there is an endothermic peak with $T_{\text{peak DSC}} = 841.4^\circ\text{C}$. The magnitude of the peak on the DSC curve, correlated with mass variation, may also indicate the presence of a physical phenomenon.

With the start of heating of magnesium stearate (StMg), in the temperature range $51-130^\circ\text{C}$, the TG curve shows a mass loss ($\Delta m = 5.00\%$), which corresponds to the dehydration process. Water loss is a process of endothermic nature, highlighted by the appearance of a high peak characteristic on the DSC curve, and $T_{\text{peak DSC}} = T_{\text{peak DTG}} = 94.1^\circ\text{C}$. With dehydration, the melting process also takes place, which usually overlaps with dehydration or even moves to lower temperatures. In this case, the corresponding well defined peak ($T_{\text{peak DSC}} = 114.8^\circ\text{C}$) due to the presence of the dehydration peak appears as a larger shoulder to the right of the latter.

In the range of $130-285^\circ\text{C}$, two extremely small endothermic peaks at 198.1°C and 274.6°C are present on the DSC curve due to the *impurities* existing as magnesium palmitate and others with higher melting temperatures. Within this range there is also a very small variation (decrease) in mass ($\Delta m = 1.00\%$).

The thermal decomposition of magnesium stearate takes place in a single step, corresponding to the range $285 - 607^\circ\text{C}$, but in the form of a very complex process, evidenced by the DSC curve, by the presence of a large number of different peaks as a thermal effect.

The DTG curve shows a high peak ($T_{\text{peak DTG}} = 382.9^\circ\text{C}$) and a total mass loss of 86.00%. As mentioned, on the DSC curve there are a series of endothermic peak, significant in size at the following temperature: 344.4°C , 388.1°C , respectively 414.8°C .

After the largest part of StMg ($\Delta m = 80.00\%$) was decomposed, a series of processes of exothermic nature took place due to the appearance of a large exothermic peak ($T_{\text{peak DSC}} = 537.0^\circ\text{C}$) preceded by three small exothermic peaks so-called shoulders), at temperatures: 429.6°C ; 459.2°C and 482.2°C . Mass loss in this last interval ($415 - 607^\circ\text{C}$) is 6.00%. The residual mass is 8.00%.

TG/DTG and DSC curves of the pure VALS and the 1:1 drug:excipient physical mixture are shown in figures 6, 7 and 8.

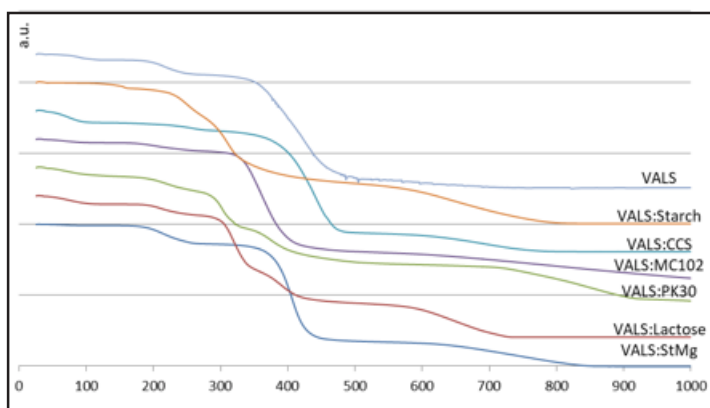


Fig. 6. TG curves of pure VALS and the 1:1 drug:excipient physical mixture

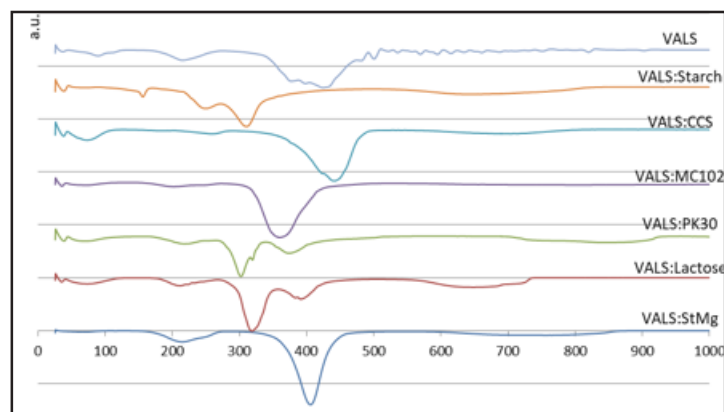


Fig. 7. DTG curves of pure VALS and the 1:1 drug:excipient physical mixture

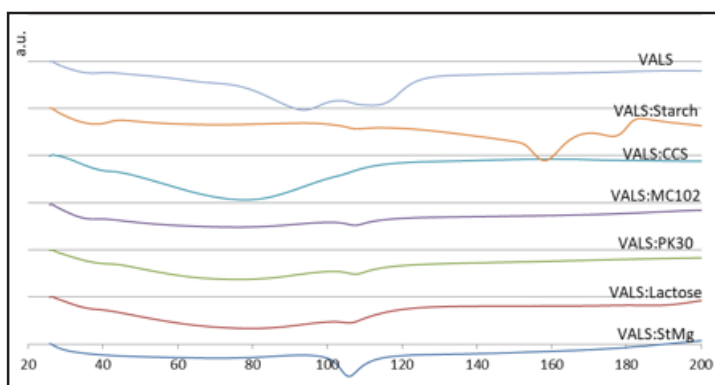


Fig. 8. DSC curves of pure VALS and the 1:1 drug:excipient physical mixture

In the 1:1 physical mixtures when there is no any interaction between drug and excipient, the T_{peak} value of melting event (DSC curve) and the first stage of the decomposition (T_{onset} and T_{peak} of TG/DTG curves) should remain practically unchanged, similarly when the drug is alone. In this case the thermal profiles of the mixture can be considered as a superposition of the curves of VALS and excipients. In the DSC curve the T_{peak} value of melting of the drug is alone, or in its mixtures when there is no interaction between drug and excipient.

According to the thermal curves (figs. 6-8), in particular the DSC curves that provide the most complete information, differences were found to be higher or lower (in the case of mixtures with starch, povidone K30, lactose monohydrate and magnesium stearate) melting temperature values, melting enthalpy values and thermal decomposition ranges. In principle, all other excipients exhibit some small but melting differences with respect to the melting temperature, respectively the value of the melting enthalpy (table 1). These differences may be due to small interactions that have not been confirmed by FT-IR spectroscopy and X-ray diffraction (XRPD).

In the case of the VALS starch mixture, the DSC curve of the VALS:starch 1:1 mixture of compared to the VALS DSC curve shows a very small, almost insignificant peak at about the same temperature as that corresponding to the melting temperature of the VALS. Practically, the so-called melting peak appears as a very small shoulder to the right of the dehydration peak, shifted to a lower temperature.

The very low-to-disappearance dimensions of the VALS melting peak, which is confirmed by the extreme low value of ΔH_{fusion} (table 1), indicate a strong chemical interaction of VALS with starch. The so-called peak present in the DSC curve is probably due to VALS residues after mixing.

The TG/DTG curves of this binary mixture showed that the beginning of the decomposition step of VALS was shifted towards a lower temperature. The values observed to this temperatures are $T_{\text{onset}} = 218; 354$ and 496 °C lower than the values obtained to the corresponding event in TG/DTG curves of VALS alone (table 1). Also, $T_{\text{peak DTG}}$ are with approximately 100 °C lower (table 1). These modifications of the temperature's values showed a reduction of thermal stability for VALS in the presence of starch, due to the mentioned interaction.

The DSC curve of the physical mix of VALS with PK30 shows a broad and strong peak corresponding to dehydration between 25 and 113 °C with $T_{\text{peak DSC}} = 75.0$ °C. The main characteristic of the DSC curve is the disappearance of the characteristic melting peak of VALS.

The disappearance of the characteristic peak for VALS melting is an indication of a chemical interaction between these substances due to heating. The rationale for this behaviour can be due to the lower temperature change of the VALS peak, which could fuse with the water loss peak of PK30 (25 - 113 °C). Another possibility is the one that includes all the water removed from the PK30, resulting in the dissolution of the VALS, due to which the VALS peak disappears.

Such behaviour has been described in the literature for PK30 mixtures with other drug substances such as naproxen, ketoprofen, ibuprofen, sodium diclofenac, acetylsalicylic acid, indicating the occurrence of a solid-solid interaction with heating. It is believed that this mode of interaction takes place by the so-called dissolution of VALS in the presence of humidity and heating.

The TG/DTG curves of the binary mixture showed that the start of the VALS decomposition step ($T_{\text{onset}} = T_i$) was shifted to a lower temperature. The observed value for this temperature is lower than the corresponding VALS decomposition temperature (table 1). In the same way, DTG peak temperatures are also modified. Currently, the movement is due to a structural change and indicates interaction, i.e. incompatibility between VALS and PK30.

Also, these changes in temperature values show a reduction in thermal stability for VALS in the presence of PK30, due to the interaction mentioned.

The DSC curve of the physical mixture of VALS with lactose monohydrate presents a broad and weak peak which corresponds to the elimination of the adsorbed water, between 41 - 94 °C with $T_{\text{peak DSC}} = 66.7$ °C. This event is followed by a broad and strong peak which correspond to the elimination of the crystallisation water between 94 - 167 °C ($T_{\text{peak DSC}} = 154.0$ °C). The main finding of the DSC curve is practically the disappearance of the characteristic VALS fusion peak.

Practically, the DSC curve has a very small, almost insignificant peak, at about the same temperature as the corresponding melting temperature of the VALS. This so-called melting peak appears as a very small shoulder to the left of the crystallization water removal peak. The very low-to-disappearance dimensions of the VALS melting

peak, which is confirmed by the very low value of ΔH_{fusion} (table 1), indicate a strong chemical interaction of VALS with α -lactose due to heating.

Regarding the TG/DTG curves it is found that the beginning of the decomposition steps of the VALS is shifted to lower temperatures. The values observed at these temperatures are $T_{\text{onset}} = 167$; 268 and 481 °C lower than those obtained with VALS alone: 309 and 544 °C (table 1). Also, $T_{\text{peak DTG}}$ is about 90 - 100 °C lower (table 1). As in previous cases, moving these temperatures to lower values reduces the thermal stability of VALS.

By comparing the DSC curves of VALS pure and StMg to those of a 1:1 physical mixture, the differences are quite visible and can be attributed to an incompatibility (interaction) between the two components.

The endothermic peak corresponding to the VALS melt disappears and a new one appears overlapping with the so-called double peak corresponding to the dehydration and StMg melting (92.6 and 107.4 °C), which is slightly shifted to lower temperatures than the StMg peak. Under these circumstances, the ΔH_{fusion} value will be higher.

A further explanation for this interaction is that StMg used is a mixture of magnesium salts of different fatty acids (mostly stearic acid and palmitic acid, respectively, other low fat acids), whose melting temperature is lower.

In literature, such interactions of StMg with drug substances such as atenolol, captopril, ibuprofen, ketoprofen, sodium diclofenac, acetylsalicylic acid, etc. are reported in literature.

Regarding the influence of StMg on the TG/DTG curves, it is manifested in the same way as in the above cases.

In accordance with the values (especially T_i and ΔH_{fusion}) from table 1, on establish that, generally, the melting peak of VALS was preserved and the enthalpy's values are reduced to half, less for the four binary mixtures mentioned. The slight lowering and/or broadening of the melting temperature, respectively beginning and maximum temperature of decomposition may be attributed to the mixing process, which lower the purity of each component in the mixture.

Appreciably decreasing or the absence of the melting temperature, respectively values of ΔH_{fusion} , suggests a process which takes place with low intensity or even disappears (the case of binary mixture VALS-PK30).

A higher value of ΔH_{fusion} shows an overlapping of two processes (the case of binary mixture VALS-StMg, with melting and dehydration).

Table 1
THERMOANALYTICAL DATA FOR VALS AND EXCIPIENTS

Samples	DSC		ΔH_{fusion} (Jg ⁻¹)	DTG		Δm (%)
	$T_{\text{onset}} /$ (fusion) °C	$T_{\text{peak}} /$ (fusion) °C		$T_{\text{onset}} /$ °C	$T_{\text{peak}} /$ °C	
<i>Drug</i>						
VALS	104.3	113.9	386.2	25 ; 174 309 ; 544	68 ; 216 403 ; 744	1.1 ; 12.7 68.9 ; 17.3
<i>Drug/excipient</i>						
Starch	108.0	114.7	32.4	25 ; 178 268 ; 354 ; 496	67 ; 206 315 ; 390 ; 644	6.3 ; 7.2 40.3 ; 21.3 ; 24.9
SiO ₂	108.0	115.4	117.3	25 ; 158 246 ; 338 ; 612	70 ; 219 303 ; 374 ; 855	6.5 ; 9.0 27.8 ; 25.7 ; 24.9
CM102	105.0	112.4	183.5	25 ; 135 274 ; 496	67 ; 201 359 ; 720	2.5 ; 6.1 70.9 ; 18.9
PK30*	*	*	*	25 ; 126 288 ; 524	71 ; 259 437 ; 696	8.1 ; 5.9 73.0 ; 13.0
α -lactose	102.1	113.2	34.6	25 ; 95 167 ; 268 ; 481	37 ; 147 246 ; 306 ; 637	0.9 ; 2.9 20.0 ; 46.9 ; 29.2
STMg**	108.0	115.4	363.7	25 ; 170 279 ; 520	85 ; 214 376 ; 424 ; 662	4.3 ; 10.9 73.0 ; 6.2

The small variations in the enthalpy's values for the binary mixtures can be attributed to some heterogeneity in the small samples used for the DSC experiments (3-4 mg).

The difference of enthalpy for the binary mixture VALS-SiO₂ can suggest a physical interaction which not determines an incompatibility.

FT-IR spectroscopy

The FT-IR spectroscopy was used as a supplementary technique in order to investigate the possible chemical interaction between drug and excipient and to confirm the results obtained by the thermal analysis. It is the most suitable technique of the non-destructive spectroscopic methods and has become an attractive method in the analysis of pharmaceutical solids, since the materials are not subject to thermal or mechanical energy during sample's preparation, therefore preventing solid-state transformations. The appearances of new absorption

band(s), broadening of band(s), and alteration in intensity are the main characteristics to evidence interactions between drug and excipients.

The FT-IR spectra were drawn for VALS, excipients, respectively for the corresponding mixtures.

For the binary mixtures which present compatibility according the DSC results, the FT-IR spectra can be considered as the superposition of the individual ones without absence, shift or broadening in the vibration bands of VALS. So, it confirms the absence of physical or chemical interactions between VALS and the corresponding excipients.

Further, it will be presented only the spectra for the cases where the thermal analysis indicates a possible interaction, namely: VALS, starch, povidone K30, lactose monohydrate and magnesium stearate, respectively the corresponding mixture of VALS with each excipient mentioned (fig. 9 - 12).

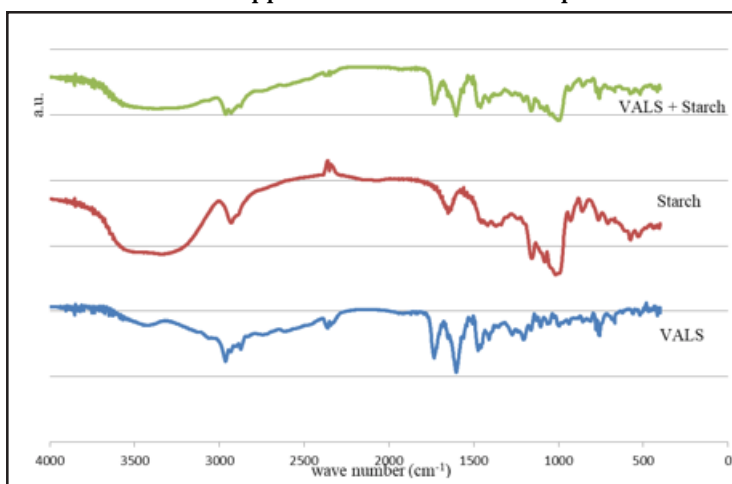


Fig. 9. IR spectra of VALS, Starch and 1:1 blend as simple mixture of VALS and Starch.

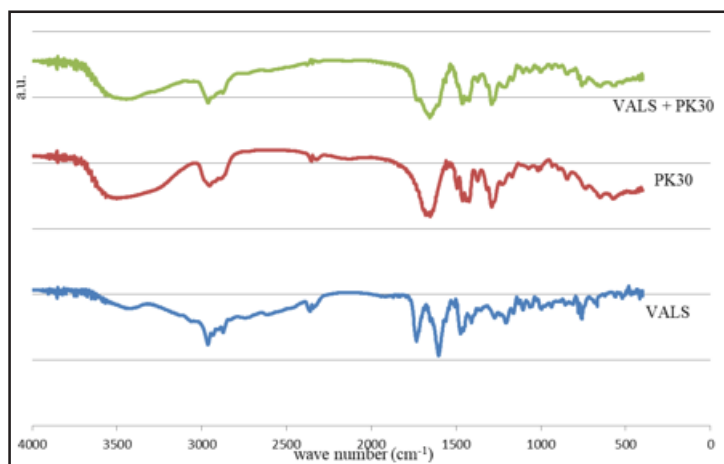


Fig. 10. IR spectra of VALS, PK30 and 1:1 blend as simple mixture of VALS and PK30.

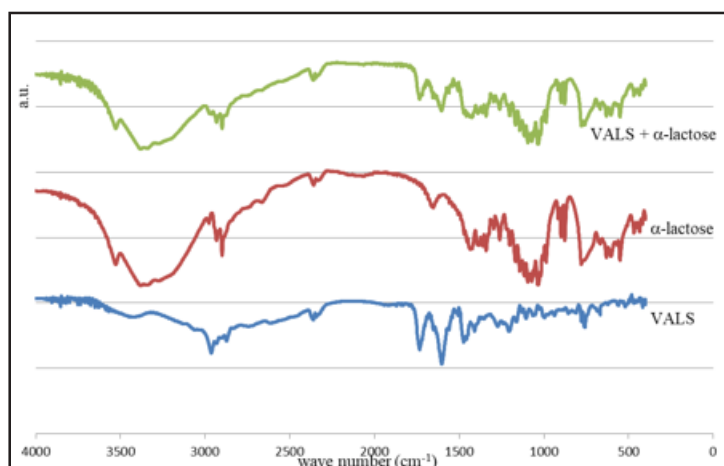


Fig. 11. IR spectra of VALS, α-lactose and 1:1 blend as simple mixture of VALS and α-lactose.

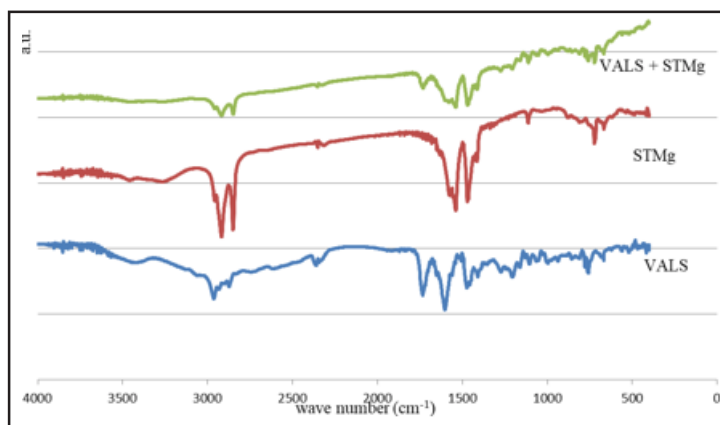


Fig. 12. IR spectra of VALS, StMg and 1:1 blend as simple mixture of VALS and StMg.

The VALS spectrum was in accordance with the literature, which in the region of 3600 - 3350 cm^{-1} describes a weak and large band (the maximum at 3426 cm^{-1}) attributed to the O-H stretching vibration (carboxyl group) as well as to the N-H stretching vibration. In the region 3000 - 2600 cm^{-1} , at 2965; 2874; 2745 and 2616 cm^{-1} , are observed four bands intensity medium which correspond to asymmetric, respectively symmetric C-H stretching vibration (from: CH_3 ; CH_2). A band of medium intensity appears at 1732 cm^{-1} and is characteristic to the C=O stretching vibration. The most intense band appears at 1603 cm^{-1} and corresponds to the C=N and C=C stretching vibration.

The two bands from the region 1470 - 1410 cm^{-1} correspond to the COO^- (asymmetric, respectively symmetric) vibrations, respectively C-C ring stretching and N=N vibrations. In the region 1280 - 1160 cm^{-1} , appear three bands of medium intensity at 1274; 1206 and 1165 cm^{-1} , that correspond to the C-H ($\delta_{\text{asym.}} \text{CH}_3$; CH_2 ; CH and $\delta_{\text{sym.}} \text{CH}_3$; CH_2 ; CH) and C-N vibrations. The four bands of weak intensity, at 1105; 1057; 997 and 939 cm^{-1} correspond to the C-O ($\nu_{\text{C-C-O}}$; $\nu_{\text{C-C(=O)-O}}$) and C-C vibrations, respectively in plane and out plane C-H bending. The bands at 816 and 758 cm^{-1} correspond to the out-of-plane C-H bending from phenyl ring. The weak bands in the region of 677 cm^{-1} corresponds to the out-of-plane C=C bending from phenyl ring, to the out-of-plane N-H bending and to the out-of-plane O-H bending. In the region of 565 - 515 cm^{-1} , the bands which appear correspond to the out-of-plane C-H bending from benzene substituted.

The spectrum of the starch presents a medium and large band in the region 3600-3100 cm^{-1} (the maximum at 3363 cm^{-1}) which corresponds to OH group from the hydration water as well as from the starch molecule. The band of medium intensity at 2932 cm^{-1} is attributed to the C-H stretching vibration from the methylene group. In the region of 1645 cm^{-1} is present a weak band, which correspond to the C-O (from ether) stretching vibration. The range of 1427-1360 cm^{-1} corresponds to the O-H bending vibrations (in plane). The bands from 1157 and 1080 cm^{-1} of medium intensity, respectively from 1016 cm^{-1} of medium-strong intensity, correspond to the C-O (C-C-O) stretching vibration, respectively to the in-plane C-H bending from ring. In the region of 930 - 710 cm^{-1} there are four bands of weak intensity which correspond to the out-of-plane C-H bending from ring. The bands from 575 and 525 cm^{-1} of weak intensity correspond to the out-of-plane C-H bending from ring substituted.

For the binary mixture, it shows the following differences:

- the significant increase ($\approx 50\%$) of the band attributed to the OH and NH groups (3426 cm^{-1}) from the VALS spectrum, with the movement of the absorptions maximum at 3371 cm^{-1} ;

- it appears a doublet at 2963 and 2932 cm^{-1} instead of the bands from 2965; 2874; 2745 and 2616 cm^{-1} (VALS) and 2932 cm^{-1} (starch);
- the disappearance of the band at 1645 cm^{-1} from starch spectrum;
- the disappearance of the bands from 1273 cm^{-1} (VALS) and 1016 cm^{-1} (starch);
- the movement of the bands from 1105 and 1059 cm^{-1} at 1082 (VALS), respectively 1049 cm^{-1} and the increase of the intensity with $\approx 60\%$, respectively $\approx 65\%$;
- the significant increase ($\approx 80\%$) of the intensity for the band from 997 cm^{-1} (VALS);
- the disappearance of the band at 677 cm^{-1} from the VALS spectrum.

The FT-IR spectrum for the physical mixture between VALS and starch suggests some chemical interactions

In respect of the povidone K30, it presents the following bands, at:

- 3507 cm^{-1} - a large band (3600 - 3100 cm^{-1}) at medium intensity, attributed to the OH group from the crystallisation water;
- 2955 cm^{-1} - a band of medium intensity, which corresponds to the C=O bending;
- 1661 cm^{-1} - a band of strong intensity as a triplet that corresponds to the carbonyl amidic group;
- 1495; 1464; 1423 cm^{-1} - these correspond to asymmetrical and symmetrical vibrations of C-H from CH_2 and CH groups;
- 1290; 1229; 1171 cm^{-1} - that correspond to the in plane and out-of-plane C-H bending;
- 845; 737; 650 cm^{-1} - these correspond to out-of-plane C-H (ring);

For the binary mixture, it shows the following differences:

- the broadening of the band at 3426 cm^{-1} (VALS) and the increase ($\approx 60\%$) in intensity;
- the medium band at 1732 cm^{-1} from VALS's spectrum disappears;
- the most intense band (1661 cm^{-1}) from the PK30's spectrum on movements at 1655 cm^{-1} ;
- the most intense band (1603 cm^{-1}) from the VALS's spectrum disappears;
- the bands at 1470 and 1410 cm^{-1} from VALS's spectrum, respectively at 1495; 1464 and 1423 cm^{-1} from PK30's spectrum appear as a strip at 1464 cm^{-1} accompanied by a doublet on the right, at 1443 cm^{-1} and 1423 cm^{-1} .
- the bands from the range: 1273 - 816 cm^{-1} (VALS) and 1229 - 844 cm^{-1} (PK30) are reduced in number and they are in the form of a wide band with multiple maximum;
- also the bands from 758 - 515 cm^{-1} range (VALS) and 737 - 575 cm^{-1} (PK30) do not return to baseline in the case of the mixture, forming a band almost as wide at the top as the base.

The FT-IR spectrum for the physical mixture between VALS and PK30 suggests some chemical interactions.

The spectrum of lactose monohydrate (α -lactose) shows a sharp medium band at 3528 cm^{-1} due to the vibration of O-H band of crystallisation water. The main bands appear at:

- 3380 cm^{-1} , as strong and large band ($3500 - 3000\text{ cm}^{-1}$) stretching vibration: intermolecular hydrogen bonded;
- a doublet at 2934 and 2901 cm^{-1} that corresponds to the C-H (CH_2) stretching vibrations;
- the range of $1435 - 1341\text{ cm}^{-1}$ corresponding to the O-H bending vibrations (in-plane);
- the range of $1261 - 1036\text{ cm}^{-1}$ which characterises the stretching vibrations C-O (in fact C-O-C and the in plane C-H bending vibrations);
- 899 ; 876 and 779 cm^{-1} that correspond to the out-of-plane C-H bending vibration;
- 633 ; 604 and 552 cm^{-1} which correspond to the O-H bending vibration (out-of-plane).

For the binary mixture with α -lactose, there were showed the following differences:

- the disappearance of the bands 3426 ; 2965 ; 2874 ; 2745 and 2616 cm^{-1} , for the VALS spectrum;
- the bands at 3426 cm^{-1} (VALS), respectively 3381 cm^{-1} (α -lactose) are greatly enlarged, corresponding to the $3650 - 2500\text{ cm}^{-1}$ range;
- the significant decrease ($\approx 40\%$) of the bands at 1732 , respectively 1603 cm^{-1} from the VALS spectrum;
- the bands from $1470 - 515\text{ cm}^{-1}$ corresponding to VALS, respectively those from $1435 - 434\text{ cm}^{-1}$ corresponding to α -lactose, are grouped into three areas: $1425 - 1034\text{ cm}^{-1}$; $1034 - 760\text{ cm}^{-1}$ and $760 - 438\text{ cm}^{-1}$, from which the last two in particular are in the form of two wide bands with a low number for so-called maximum and a lot of shoulders. For most of the maximums, the intensity is not significantly reduced.

Based on the submitted aspects one can sustain chemical interactions between VALS and α -lactose.

Magnesium stearate presents a weak an large band in the region $3600 - 3100\text{ cm}^{-1}$ (the maximum at 3264 cm^{-1}). At 2918 and 2851 cm^{-1} , there were observed two sharp

bands with maximum absorbtion due the C-H vibrations from CH_2 - CH_3 group. In the $1576 - 1472\text{ cm}^{-1}$ region, are showed asymmetric, respectively symmetric stretching vibrations corresponding to the carboxyl anion.

Other bands that must be maintained have their peaks at 2957 cm^{-1} corresponding to the asymmetrical vibration of C-H band in methyl group, respectively those at 721 cm^{-1} which correspond to *rocking* deformation (H-C-H); $n > 3$.

The FT-IR spectrum of VALS-StMg mixture shows the following changes:

- the disappearance of the band from the region $3600 - 3100\text{ cm}^{-1}$;
- the four bands from the VALS spectrum (at: 2965 ; 2874 ; 2745 and 2615 cm^{-1}), respectively the two bands from the StMg spectrum (at 2918 and 2851 cm^{-1}) are reduced at a doublet at 2918 and 2851 cm^{-1} and the intensity decrease with $\approx 50-80\%$;
- the significant decrease ($\approx 60\%$) of the band from 1732 cm^{-1} ;
- the disappearance of the most intense band (1603 cm^{-1}) from VALS spectrum;
- the significant decrease ($\approx 60\%$) of the intensity for the bands from the region 1576 ; 1539 and 1472 cm^{-1} in the StMg spectrum;
- the decrease ($\approx 50\%$) of the intensity for the most intense bands from the region $810 - 670\text{ cm}^{-1}$ (758 and 723 cm^{-1}).

On the bases of mentioned differences it may be considered that the VALS interacts with StMg and the appearance of the obtained products from the chemical interaction (the magnesium salt of VALS and free stearic acid).

To investigate the possible interaction of VALS with the four excipients mentioned, besides the FT-IR spectroscopy which is a qualitative analysis technique, the X-ray powder diffraction (XRPD) has been used for qualitative and quantitative identification of crystallinity. The number of the speciality articles which uses the X-ray powder diffraction is growing.

The XRPD of VALS, starch, PK30, α -lactose, StMg and of the binary mixtures are shown in figures 13-16.

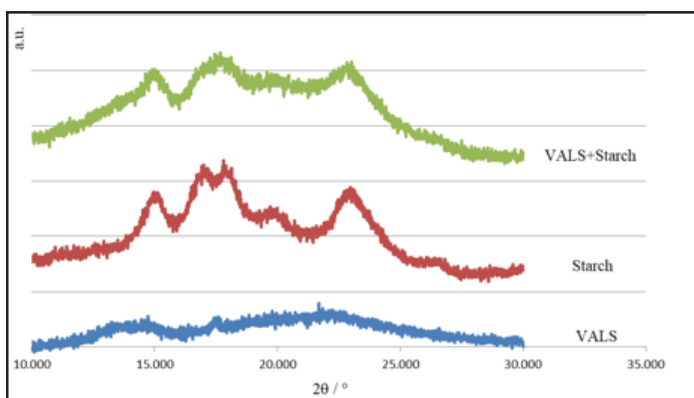


Fig. 13. X-ray diffractogram of starch, VALS and 1:1 blend as simple mixture of VALS and starch

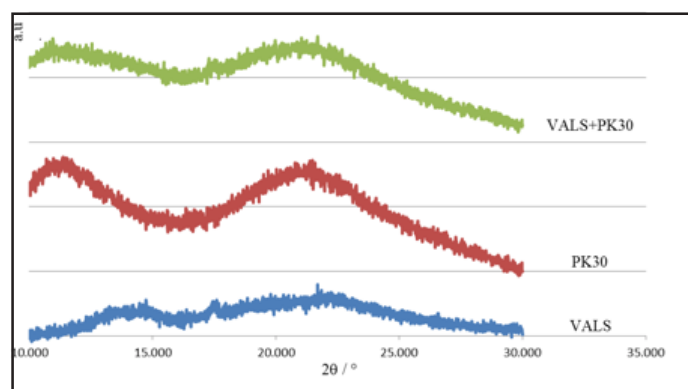


Fig. 14. X-ray diffractogram of PK30, VALS and 1:1 blend as simple mixture of VALS and PK30

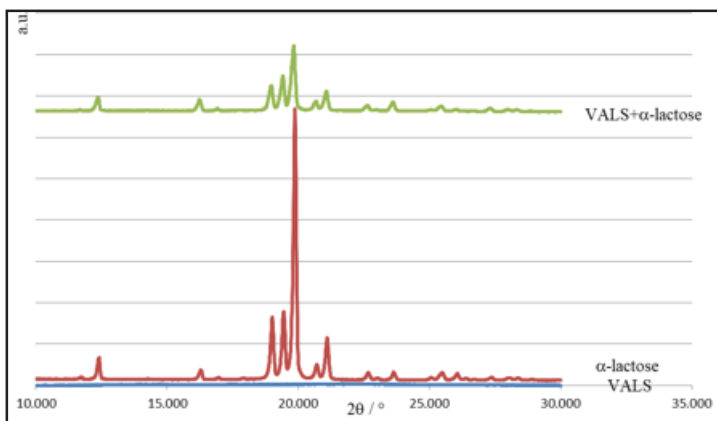


Fig. 15. X-ray diffractogram of lactose, VALS and 1:1 blend as simple mixture of VALS and lactose

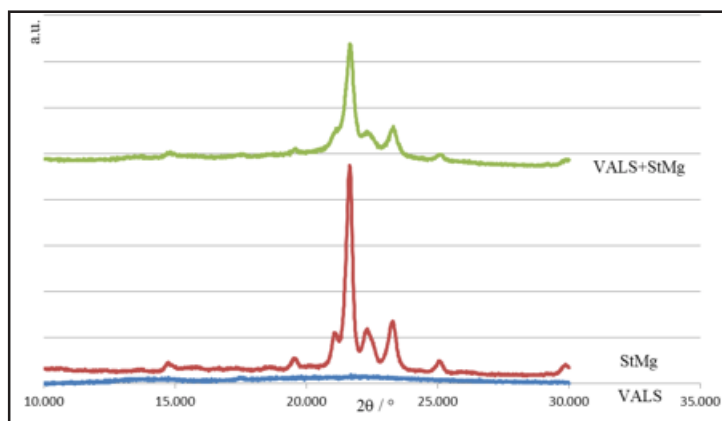


Fig. 16. X-ray diffractogram of StMg, VALS and 1:1 blend as simple mixture of VALS and StMg

VALS		VALS + Starch		Starch	
2θ	I%	2θ	I%	2θ	I%
14.740	70.45177	14.82	90.71038	11.92	53.64121
17.450	67.60584	17.45	100	16.93	96.80284
18.840	73.92024			17.81	100
19.780	81.36696				
20.310	80.45783				
21.690	100				
		22.83	95.68913	22.86	84.19183
26.580	43.11695				

Table 2
X-RAY DIFFRACTION
DATA FOR VALS,
STARCH AND VALS-
STARCH (1:1) MIXTURE

VALS		VALS + PK30		PK30	
2θ	I%	2θ	I%	2θ	I%
		10.96	99.77029		
14.740	70.45177			11.38	100
17.450	67.60584				
18.840	73.92024				
19.780	81.36696				
20.310	80.45783				
21.690	100	21.68	100	21.38	98.27791
26.580	43.11695				

Table 3
X-RAY DIFFRACTION
DATA FOR VALS, PK30
AND VALS-PK30 (1:1)
MIXTURE

VALS		VALS + α-lactose		α-lactose	
2θ	I%	2θ	I%	2θ	I%
14.740	70.45177	12.34	22.49432		
		16.21	19.08795		
17.450	67.60584				
18.840	73.92024	18.95	41.0483	19.01	23.44745
		19.4	54.35463	19.44	25.55492
19.780	81.36696	19.82	100	19.87	100
20.310	80.45783	20.63	16.22169		
		21.07	32.25925	21.1	15.96519
21.690	100				
		23.57	14.94507		
26.580	43.11695				

Table 4
X-RAY DIFFRACTION
DATA FOR VALS,
LACTOSE AND VALS-
LACTOSE (1:1)
MIXTURE

VALS		VALS + StMg		StMg	
2 θ	I%	2 θ	I%	2 θ	I%
14.740	70.45177				
17.450	67.60584				
18.840	73.92024				
19.780	81.36696				
20.310	80.45783				
21.690	100	21.65	100	21.64	100
				22.3	24.68875
		23.32	37.26137	23.27	28.52923
26.580	43.11695				

Table 5
X-RAY DIFFRACTION
DATA FOR VALS, StMg
and VALS-StMg (1:1)
MIXTURE

The additional prominent DSC peaks in the mixtures of the drugs and excipients are a positive indication of chemical interaction of the drugs with excipients. Such interaction should result in the partial or complete disappearance of the reactant phases and appearance of new phases, which can be inferred from XRPD. X-ray diffraction patterns of the mixture, prepared at room temperature, when compared with those of its individual components showed appearance of new lines and disappearance of some of the lines present in the individual components.

The X-ray patterns of VALS-starch, respectively VALS-StMg mixtures prepared at room temperature did not show the lines in addition to those present in patterns of the individual components (tables 2 and 5). However, the number of lines present in the XRD patterns of the individual components was found missing in the similar pattern recorded for the mixture. The significant difference in the X-ray patterns of the drug-excipient mixtures compared to those of individual drugs and excipient indicates possible incompatibility of the drugs with the excipient, even at room temperature. The presence of majority of the lines of the parent substances in the thoroughly ground mixture prepared at room temperature, however, suggests the interaction of the drug with the excipient at room temperature, which could increase with the increased temperature.

The number of new lines appeared in VALS-PK30, respectively VALS-lactose monohydrate mixtures are shown in tables 3 and 4. The same tables indicate disappearance of some of the diffraction lines of higher, moderate and lower intensities in the mixture which are originally present in the X-ray diffraction patterns of the individual components which indicates the interaction of VALS with PK30 and lactose monohydrate.

Conclusions

In this article, a major problem has been addressed, commonly found in specialized literature, such as the compatibility and stability of drug substances with various excipients. Thus, the stability and compatibility of VALS with a number of excipients mentioned in the article was studied. As studio methods were used: thermal analysis methods, FT-IR spectroscopy and X-ray diffraction patterns (XRPD).

The results confirmed that thermal analysis is an effective and reliable technique in the compatibility studies of drug-excipient mixtures. Moreover, the DSC technique offers significant advantages, so that it is considered as a fast screening tool for drug-excipient interaction in a preformulation process.

The changes in the profile of thermoanalytical curves (TG/DTG/DSC) in the case of some binary mixtures indicate the production of some interactions as a function of heating.

According to the thermal curves, especially DSC curves, one can say that all tested excipients present lower or

higher interactions with VALS. This fact is supported by the differences between the values of T_{fusion} and of the enthalpies of melting.

Considering that the enthalpies of melting are quantitative data since they may be expressed as a fractional change, it could be said that starch, PK30, α -lactose and StMg certainly interact chemical with VALS. In the same context, the CCS interaction occurs in a certain extent, whilst other excipients interaction is unlikely.

The interaction of starch, PK30, α -lactose and StMg with VALS was confirmed by FT-IR spectroscopy and by XRPD. In terms of CCS interaction with VALS, this was not confirmed by the two techniques mentioned, probably because of limited modifications.

This study shows the incompatibility of VALS with starch, PK30, α -lactose and StMg.

References

- VIERECK J, KUMARSWAMY R, FOINQUINOS A, XIAO K, AVRAMOPOULOS P, KUNZ M, DITTRICH M, MAETZIG T, ZIMMER K, REMKE J, *Sci Transl Med* **8**, 2016, p. 326
- THAO TRUONG-DINH TRAN, PHUONG HA-LIEN TRAN, JUN-BOM PARK, AND BEOM-JIN LEE, *Arch Pharm Res* **35**, 2012, p. 1223
- CHAPLIN S, *Prescriber*, **27**, 2016, p. 56
- HOWELL B.A., RAY J.A., *J. Therm. Anal. Cal.*, **83**, 2006, p. 63
- HOWELL B.A., *J. Therm. Anal. Cal.*, **85**, 2006, p. 165
- GAO M-J, DING X-L, HU Q-CH., *Thermochim Acta.*, **525**, 2011, p. 1.
- DRAGOMIROIU G.T.A.B., GINGHINA O., MIRON D.S., BARCA M., POPA D.E., HIRJAU M., LUPULEASA D., RADULESCU E.S., *Farmacia*, **63(2)**, 2015, p. 280.
- SOOD J., SAPRA B., TIWARY A.K., *AAPS PharmSciTech*, **18(6)**, 2017, p. 1901.
- HANGAN A.C., TURZA A., STAN R.L., STEFAN R., OPREAN L.S., *Russian Journal of Coordination Chemistry*, **41(6)**, 2015, p. 365.
- KLIMOVA K, LEITNER J, *Thermochim Acta.*, **550**, 2012, p. 59.
- FULIAS A., TITA B., BANDUR G., TITA D., *Rev. Chim. (Bucharest)*, **60**, no.10, 2009, p. 1079.
- FITA C.A., LUPULIASA D., HIRJAU V., SALA G., KARAMPELAS O., SARAMEG G., *Farmacia*, **60(6)**, 2012, p.905.
- DEDIU V., MUSAT V., JURCA B., CRISTEA N.I., *Rev. Chim. (Bucharest)*, **68**, no.8, 2017, p. 1703.
- IORDACHE S, TUTUNARU B, SAMIDE A, POPESCU A, *Rev. Chim. (Bucharest)*, **70**, no.2, 2019, p. 503.
- BANCUTA O. R., CHILIAN A., BANCUTA I., SETNESCU R., SETNESCU T., ION R.M., *Rev. Chim. (Bucharest)*, **69**, no.6, 2018, p. 1346.
- MOISEI A., GLIGOR E., BOJITA M., CHIS A., TOTAN M., VONICA-GLIGOR L.A., CIURBA A., *Farmacia*, **62(6)**, 2014, p. 1239.
- NITA A., TIT D.M., COPOLOVICI L., MELINTE C.E., CARMEN E., COPOLOVICI D.M., BUNGĂU S., IOVAN C., *Rev. Chim. (Bucharest)*, **69**, no. 2, 2018, p.297.
- TITA B., MARIAN E., FULIAS A., JURCA T., TITA D., *J Therm Anal Calorim.* **112**, 2013, p. 367.
- TITA B., STEFANESCU M., TITA D., *Rev. Chim. (Bucharest)*, **62**, no.10, 2011, p. 1002.
- TITA B., FULIAS A., STEFANESCU M., MARIAN E., TITA D., *Rev. Chim. (Bucharest)*, **62**, no.2, 2011, p.216.
- TITA D., JURCA T., TITA B., *J Therm Anal Calorim.* **111**, 2013, p. 291.

Manuscript received:15.10.2018